# Mobilities of Mass-Identified $H_3^+$ and $H^+$ Ions in Hydrogen*†

D. L. ALBRITTON,‡ T. M. MILLER, D. W. MARTIN, AND E. W. MCDANIEL
*School of Physics, Georgia Institute of Technology, Atlanta, Georgia*
(Received 27 November 1967)

The drift velocities of mass-identified $H_3^+$ and $H^+$ ions in hydrogen gas at room temperature were measured. The $H_3^+$ ions were found to be in thermal equilibrium with the gas at $E/p_0$ less than about 10 V/cm Torr; the $H^+$ ions, at $E/p_0$ less than about 5 V/cm Torr. From these measurements, the reduced zero-field mobilities were deduced: $H_3^+$, $11.1\pm0.6$ cm²/V sec; $H^+$, $16.0\pm0.8$ cm²/V sec. This investigation was performed with a long, low-pressure drift tube using a pulsed time-of-flight technique. The arrival-time histograms presented evidence of hydrogen ion–molecule reactions. It is shown that these reactions introduce no ambiguity in ascribing the above zero-field mobilities to single ionic species. Only a negligible fraction of the detected $H_3^+$ ions were formed by the three-body conversion of $H^+$ into $H_3^+$. Above an $E/p_0$ of about 54 V/cm Torr, the disruption of $H_3^+$ ions contributes substantially to the $H^+$ signal. The reactive formation of $H_5^+$ from $H_3^+$ was evident in the $H_5^+$ arrival-time histograms. The zero-field mobility of potassium ions in hydrogen was also determined, and the close agreement with the data of other investigators demonstrates that the apparatus is relatively free of unknown systematic uncertainties.

## I. INTRODUCTION

POSITIVE-ION mobility research was born in the late 1890's at the Cavendish Laboratory when J. J. Thomson, as well as Ernest Rutherford and J. S. Townsend, noted that the passage of Roentgen's newly discovered x-rays through gases, which were normally good insulators, made these gases conductive. The early recognition that these conduction currents could be attributed to "mobile" charge-bearing molecules has led to experimental and theoretical research on the motion of slow ions in gases which has continued unabated through several generations of both investigations and investigators.

Ionic mobilities are of continued interest for two reasons. Numerical values, and particularly their dependence on temperature, can throw the hard light of experiment on ion-molecule interactions at thermal energies. Secondly, the mobility constant is an important transport coefficient for weakly ionized gases.

Hydrogen, as the simplest molecular gas, has been the object of considerable mobility research. In spite of this, discrepancies exist between various sets of experimental data and the effect of reactions between the positive ions and the parent gas on these mobility data was not fully evaluated. The remainder of this paper summarizes the method and results of an investigation in which the role of ion-molecule reactions in the determination of the mobilities of mass-identified hydrogen ions in hydrogen is specifically assessed.

## II. DEFINITIONS AND CONVENTIONS

Before summarizing the status of hydrogen-ion mobility research, certain definitions of terms are in order. It has been traditional to refer to the ratio of the ionic drift velocity $v_d$ to the electric field strength $E$ as the *mobility:*

$$K_{\mathrm{op}}\equiv v_d/E. \tag{1}$$

This ratio itself is generally a complicated function of the electric field strength. Theory predicts that at vanishingly small field strengths this ratio is a constant, namely, the *zero-field mobility:*

$$\lim_{E\to 0} K_{\mathrm{op}}\equiv K. \tag{2}$$

The subscript on $K_{\mathrm{op}}$ denotes that the quantity is simply the *operational* ratio of drift velocity to field strength. Because of the difficulty of calculating a value for $K_{\mathrm{op}}$ when the electric field strength is nonvanishing, comparison between theory and experiment is simpler for the zero-field mobility $K$.

Theory also predicts that the mobility is inversely proportional to the gas number density $N$. Therefore, to facilitate comparisons between experimental data gathered at a variety of gas pressures, mobilities are customarily normalized to the gas number density at 760 Torr and 0°C. Following the notation of Dalgarno, McDowell, and Williams[1] these normalized, or *reduced mobilities* are denoted herein in script and are expressed as

$$\mathcal{K}_{\mathrm{op}}=(v_d/E)(p/760)(273/T), \tag{3}$$

where $p$ is the gas pressure in Torr and $T$ is the gas temperature in degrees Kelvin at which the ratio $v_d/E$ was obtained. The *reduced, zero-field mobility* is defined by a limit analogous to that in Eq. (2). At the gas densities of interest, the energetics of an ion-molecule interaction are characterized by the gas temperature and the ratio $E/p_0$, where $p_0$ is the normalized pressure ($p_0=p273/T$). Therefore, operational mobility data

* This research was supported in part by the Office of Naval Research in Project Squid, University of Virginia, and in part by the U. S. Air Force Office of Scientific Research.

† This paper summarizes the dissertation submitted by D. L. A. to the faculty of the Georgia Institute of Technology in partial fulfillment of the requirements for the degree of Doctor of Philosophy.

‡ Present address: Aeronomy Laboratory, ESSA Research Laboratories, Boulder, Colo.

[1] A. Dalgarno, M. R. C. McDowell, and A. Williams, Phil. Trans. Roy. Soc. London **A250**, 411 (1958).

recorded at a given temperature are customarily presented as a function of $E/p_0$ or $E/N$.[2]

## III. HISTORICAL DEVELOPMENT

The early experimental investigations of hydrogen-ion mobilities suffered in varying degrees from contaminants present in the supply gas or outgassed from the inner surfaces of the apparatus. Even small traces of such impurities can become ionized by charge-transfer and ion-molecule reactions with the hydrogen ions and may constitute a relatively large fraction of the total positive-ion signal. As a result, most of the investigations conducted before the advent of modern ultrahigh vacuum techniques and the availability of gases with impurity content less than a few parts per million are now only of historical interest.

Even in pure hydrogen, however, the identity of the drifting ions has been controversial. Electron impact on hydrogen produces $H^+$ and $H_2^+$ as primary ions, with the latter in the vast majority.[3] For many years it was assumed that $H_2^+$ was the predominant ionic species that had been observed in mobility experiments. Varney,[4] however, drew attention to the formation of $H_3^+$ by the process

$$H_2^+ + H_2 \rightarrow H_3^+ + H. \quad (4)$$

Because of the large cross section for this process, Varney concluded that the observed species was $H_3^+$.

Barnes, Martin, and McDaniel[5] experimentally confirmed Varney's hypothesis and, in addition, pointed out that $H^+$, despite the reaction

$$H^+ + 2H_2 \rightarrow H_3^+ + H_2, \quad (5)$$

can exist in measurable quantities at gas pressure common to mobility experiments. Saporoschenko[6] observed $H_5^+$ and demonstrated its three-body formation via

$$H_3^+ + 2H_2 \rightarrow H_5^+ + H_2. \quad (6)$$

The existence of $H^+$, $H_3^+$, and $H_5^+$ in mobility experiments points out the need for positive and simultaneous mass identification of the components of the hydrogen-ion signal. The first such mass-identified mobility data for hydrogen were reported by Saporoschenko.[7] The general agreement of Saporoschenko's $H_3^+$ data and those reported earlier by Rose,[8] Chanin,[9]

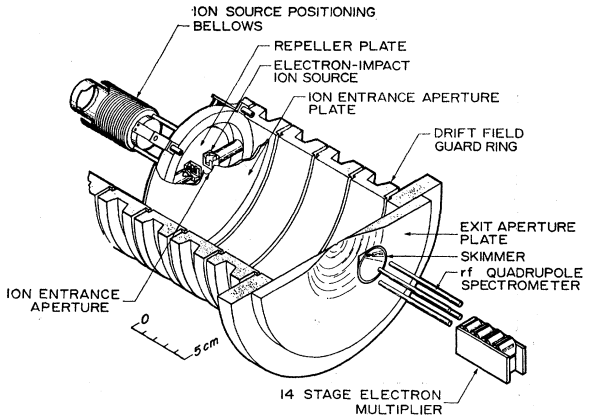


FIG. 1. A pictorial view of the drift region and the mass analysis and detection system.

Jaeger and Otto,[10] Sinnott,[11] and Dutton *et al.*[12] confirmed that the identity of the ionic species in these earlier investigations was indeed $H_3^+$. However, these sets of data differed numerically in some cases by as much as 20% and in a fashion which was often systematic. Saporoschenko also reported data for the minority $H^+$ and $H_5^+$ ions, but his data did not extend to sufficiently low $E/p_0$ to demonstrate that the operational mobility became independent of $E/p_0$ at low field strengths.

Even in pure hydrogen and with positive mass identification, a mobility measurement may still be ambiguous. Ion-molecule reactions imply that the members of a detected species may have spent fractions of their existence as ions of another type. In that case, the deduced drift velocity may not be characteristic of a single given species. For example, Eqs. (4) and (5) indicate that a detected $H_3^+$ ion may either have been created swiftly by the first reaction or may have spent a portion of the drift time as $H^+$. Similarly, Eq. (6) shows that the $H_5^+$ signal will most certainly bear some of the characteristics of that for $H_3^+$ ions.

In view of all of this, it appears that a meaningful comparison between theory and experiment for the zero-field mobility can be made only when the experimental value was obtained under the following stipulations:

(1) The ionic identity must be unequivocally determined.

(2) The data must clearly indicate that the drift velocities used to determine $\mathcal{K}_{op}$ cannot be ascribed to an ionic species which spent part of its drift time as another ionic type.

(3) It must be demonstrated that $\mathcal{K}_{op}$ is independent of $E/p_0$ at low electric field strengths; i.e., $\mathcal{K}_{op}$ constant in a "low-$E/p_0$" range.

[2] L. G. H. Huxley, R. W. Crompton, and M. T. Elford have proposed that $E/N$ be expressed in units of the "Townsend" whose magnitude is defined as 1 Townsend (Td) $\equiv 10^{-17}$ V cm$^2$. See Bull. Inst. Physics and Physical Soc. **17**, 251 (1966).
[3] W. Bleakney, Phys. Rev. **35**, 1180 (1930).
[4] R. N. Varney, Phys. Rev. Letters **5**, 559 (1960).
[5] W. S. Barnes, D. W. Martin, and E. W. McDaniel, Phys. Rev. Letters **6**, 110 (1961).
[6] M. Saporoschenko, J. Chem. Phys. **42**, 2760 (1965).
[7] M. Saporoschenko, Phys. Rev. **139**, A349 (1965).
[8] D. J. Rose, J. Appl. Phys. **31**, 643 (1960).
[9] L. M. Chanin, Phys. Rev. **123**, 526 (1961).
[10] G. Jaeger and W. Otto, Z. Physik **169**, 517 (1962).
[11] G. Sinnott, Phys. Rev. **136**, A370 (1964).
[12] J. Dutton, F. Llewellyn Jones, W. D. Rees, and E. M. Williams, Phil. Trans. Roy. Soc. London **A259**, 299 (1966).

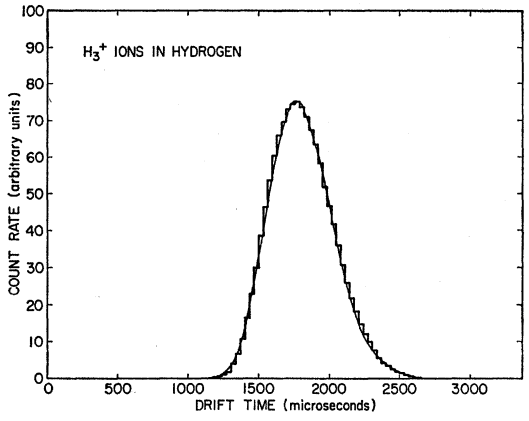


FIG. 2. A comparison of an arrival-time histogram of $H_3^+$ ions with the spectrum predicted by Eq. (7) for the following conditions: $E/p_0$ 0.52 V/cm Torr, drift distance 7.7 cm, drift velocity $0.43\times10^4$ cm/sec, pressure 0.95 Torr, temperature 304°K, and pulse width 20 $\mu$sec.

## IV. APPARATUS

Figure 1 presents a pictorial view of the essential components of the apparatus, and, with its aid, the basic properties of the method can be outlined. The movable electron-impact ion source is immersed in hydrogen gas contained within a drift tube. At one of its positions on the drift tube axis, the source creates a brief, spatially narrow group of *primary* hydrogen ions which, under the action of a weak axial electric field, migrate down the drift space. A sample of the diffusively broadened ion swarm that arrives at the remote end of the tube passes through the exit aperture and enters a differential pumping region. The conical skimmer selects the core of the emergent ion-neutral mixture for mass analysis of the ions. The ions of a selected charge-to-mass ratio are detected individually and are sorted electronically according to their arrival times.

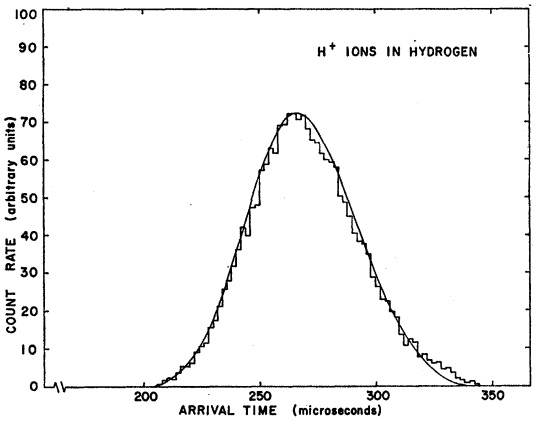


FIG. 3. A comparison of an arrival-time histogram of $H^+$ ions with the spectrum predicted by Eq. (7) for the following conditions: $E/p_0$ 3.8 V/cm Torr, drift distance 14.0 cm, drift velocity $4.6\times10^4$ cm/sec, pressure 0.15 Torr, temperature 303°K, and pulse width 1 $\mu$sec.

Only an extremely small fraction of the number of ions in each original burst negotiates the journey from source to detector. Nevertheless, by repetitive pulsing of the source, the arrivals of randomly selected members of the swarms build up a histogram, or spectrum, of arrival times, the average of which reflects the mean transit time of the given ionic species. By changing only the position of the ion source, other arrival-time spectra can be recorded. The time differences between the centroids of these spectra recorded at the different drift lengths may be taken to be the average time required by the selected ionic species to drift between source positions and are independent of end effects produced either by the source or in the mass analysis and detection system. The average drift velocity is then the ratio of the source displacement to the corresponding time difference, and the operational mobility follows.

The continuously movable, electron-impact ion source can be placed within a few thousandths of an inch at any of eight positions along the drift space axis to yield drift lengths which vary from 1–44 cm. The initial ribbon of primary ions is kept axially thin by using ionizing pulse widths that are "instantaneous" relative to the total drift time. Mutual repulsion can be held to a negligible level by using low emitted electron currents (5–10 $\mu$A) and narrow ionizing pulse widths (0.5–20 $\mu$sec). The ions depart the electron-impact source and enter the drift space through a 1.6-cm-diam knife-edged, entrance aperture.

The drift space is flanked by a set of fourteen guard rings with 17.5 cm i.d. The rings are similar to those used by Crompton, Elford, and Gascoigne[13] and maintain an axial electric field which is free of distortion to a fraction of a percent in the region traversed by the ion swarm. Concealed alumina spacers and dowel pins electrically separate the guard rings and establish alignments to a few thousandths of an inch. All surfaces exposed to the ion swarm are gold plated to reduce surface and contact potentials.

The ion sample leaves the drift space through a 0.079-cm-diam knife-edged aperture. No guiding or focussing field was used in the differential pumping region between exit aperture and skimmer, where the mean free path changes by orders of magnitude, to avoid the possibility of dissociating weakly bound ions. The 4-in. radio-frequency quadrupole mass filter[14] meets the criterion of positive mass identification imposed in the preceeding section. A nude, 14-stage electron multiplier permits the counting of individual ionic arrivals. The time interval between the creation of an ion swarm and the detection of one of its members is measured and stored by a 256-channel time-of-flight analyzer (channel widths: 0.25–64 $\mu$sec), the sweep of

[13] R. W. Crompton, M. T. Elford, and J. Gascoigne, Australian J. Phys. 18, 409 (1965).

[14] W. R. Saxton, D. B. Dunkin, F. C. Fehsenfeld, and A. L. Schmeltekopf (private communication).

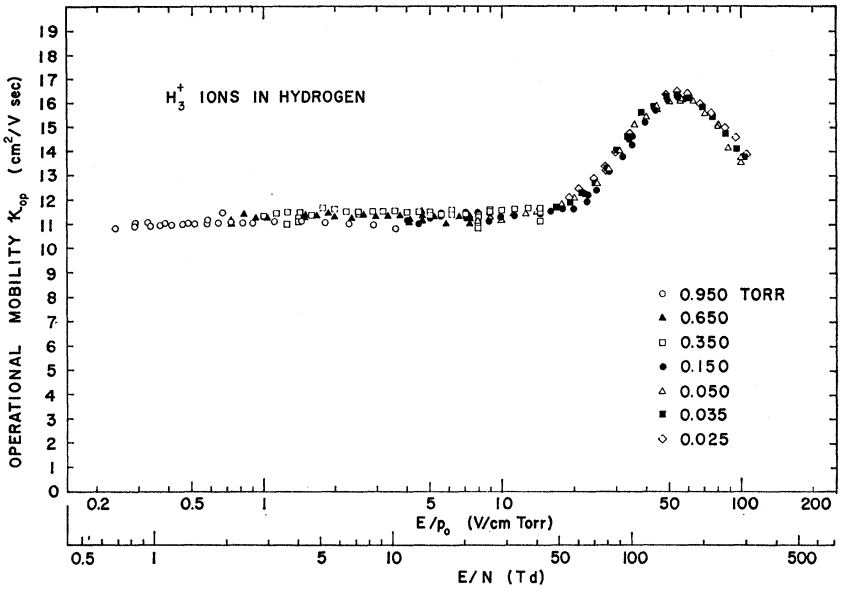


FIG. 4. Operational mobility data of mass-identified $H_3^+$ ions in hydrogen gas at 300°K (typical). 1 Townsend (Td) $\equiv 10^{-17}$ V cm².

which is triggered by the ionizing pulse of the electron impact source.

The vacuum chamber was built with strict adherence to ultrahigh vacuum techniques and is evacuated by oil diffusion pumps, baffled by molecular sieve traps. After baking the chamber for 12 h at 200°C, base vacua on the order of $10^{-9}$ Torr are achieved. The background drift tube pressure after seal-off never exceeds $5\times10^{-7}$ Torr. High-purity hydrogen is supplied by a silver-palladium diffusion tube.[15] Drift tube pressure is maintained by a servo-driven leak valve and measured by a calibrated capacitance manometer. Thermocouples attached to the exterior of three of the guard rings indicate drift space temperatures.

## V. TRANSPORT PROPERTIES

The second of the above criteria is met by a consideration of the transport behavior of the ion swarm. The experimental geometry depicted in Fig. 1 was constructed to approximate closely an idealized situation for which an analytical solution of the transport equation can be obtained. As shown in the Appendix, the time variation of the measured flux of nonreacting, thermal ions through the exit aperture of area $A$ at a distance $z$ from the source in an infinite cylindrical volume is given by

$$\varphi(0,z,t)=\frac{A\sigma_0}{4(\pi Dt)^{1/2}}(v_d+z/t)\exp\left(-\frac{(z-v_dt)^2}{4Dt}\right)\times\left[1-\exp\left(-\frac{r_0^2}{4Dt}\right)\right], \quad (7)$$

where $D$ and $v_d$ are the scalar diffusion coefficient and drift velocity of the ionic species, respectively, and $\sigma_0$ is the initial surface ion density deposited across an axially thin disk of radius $r_0$ at time $t=0$. Therefore, Eq. (7) would predict the arrival-time distribution of a primary ion swarm that was (a) instantaneously created by the electron impact source described earlier and (b) that had drifted and diffused without ion-molecule reactions under low-$E/p_0$ conditions over a given drift length.

Agreement in form between Eq. (7) and an experimental arrival-time histogram can be demonstrated in the following manner. An experimental value for $v_d$ is measured under low-$E/p_0$ conditions for a given species in the manner described in the preceding section. From the associated value of the mobility, the diffusion coefficient is taken from the relation between $D$ and K given by Eq. (9).

Figure 2 presents a comparison for $H_3^+$. An arrival-time spectrum is generated by inserting the values of $v_d$ and $D$ thus obtained into Eq. (7), and the resulting smooth curve is normalized to and aligned with the peak of the corresponding arrival-time histogram. (The shift along the $t$ axis is to remove sampling time.) Figure 3 shows a similar comparison for $H^+$ ions. A trial variation of the value of $D$ in Eq. (7) of more than about 10% from the value obtained in the fashion noted above produces a discernable misfit between these predicted and recorded widths.

Agreement between the widths of the analytical curve and the experimental histogram was very good for all of the low-$E/p_0$ cases examined for both $H_3^+$ and $H^+$, as illustrated by the examples in Figs. 2 and 3. This agreement demonstrates that the motion of the $H_3^+$ and $H^+$ ions under low-$E/p_0$ conditions was described by the assumptions leading to Eq. (7), namely, that thermal ions of a given species migrate under the

[15] J. R. Young, Rev. Sci. Instr. 34, 891 (1963).

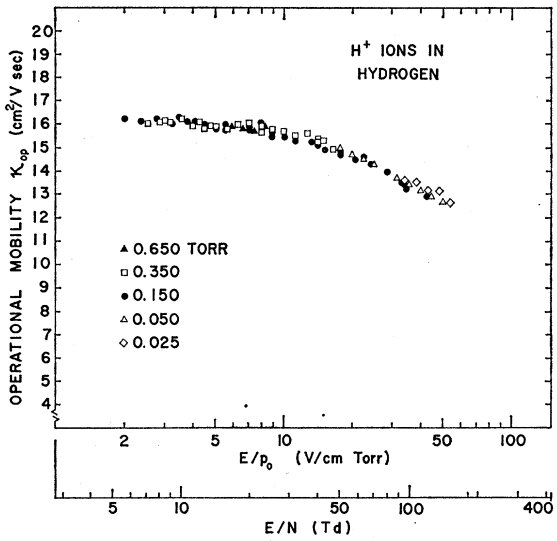


FIG. 5. Operational mobility data of mass-identified $H^+$ ions in hydrogen gas at 300°K (typical). 1 Townsend (Td) $\equiv 10^{-17}$ V cm².

action of field-engendered drift and diffusion alone and that their number is not significantly increased by additive ion-molecule reactions.

## VI. EXPERIMENTAL DATA

Drift velocity values for $H_3^+$ or $H^+$ ions at a given gas pressure and $E/p_0$ were obtained in the following manner: The channel width of the time-of-flight analyzer was selected such that, for the particular $p$, $E/p_0$, and ion source position, the arrival-time histogram would be contained in a maximum number of the 256 channels. The period of the pulsed ion source was set slightly greater than the sweep time of the multichannel analyzer. With all experimental parameters held constant, counts were accumulated until the channel in which the peak of the distribution occurred was represented by a minimum of 500 counts, a level at which noise counts and counting statistics produced only a negligible effect on the histogram. Usually, several thousand counts represented the histogram peak. As will be pointed out later, the centroid of the histogram represents the mean arrival time of the ions with only negligible error at low $E/p_0$. Measured mean arrival times varied from tens of microseconds to several milliseconds, depending on ionic type and the values of various parameters.

By recording a minimum of three (and up to seven) arrival-time histograms using different ion source positions, a set of mean arrival times $\bar{t}_i$ and corresponding drift lengths $L_i$ was obtained for a given pressure and $E/p_0$. The drift velocity was then the reciprocal of the slope of a line, fitted by least squares, to the set of $(\bar{t}_i, L_i)$. The rms deviation of the points $(\bar{t}_i, L_i)$ about the fitted line was usually about 1%.

Figure 4 shows the operational mobilities recorded as a function of $E/p_0$ for $H_3^+$ at a variety of gas pressures. Below a value of $E/p_0$ of about 10 V/cm Torr, the data gathered at a given pressure exhibit no discernable dependence on $E/p_0$, thereby satisfying the third of the above criteria. There are, however, systematic (3% max) differences between the averages of these low-$E/p_0$ data as a function of pressure, undoubtedly reflecting the $\pm 2\%$ accuracy of the pressure measurement and control system. The high-pressure measurements are believed to be more accurate; consequently, the high-pressure data were given slightly more weight in the average of the data gathered at $E/p_0 \leq 10$ V/cm Torr to determine the value of the zero-field mobility. The resulting value of $\mathcal{K}$ for $H_3^+$ is 11.1 cm²/V sec.

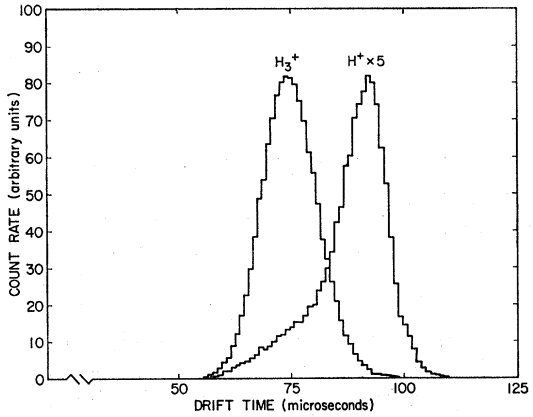


FIG. 6. A comparison between $H_3^+$ and $H^+$ arrival-time histograms recorded under the same conditions, with the latter showing contributions from the disruption of $H_3^+$ ions. Drift distance 44.8 cm, pulse width 0.9 μsec, $E/p_0$ 56 V/cm Torr, pressure 0.05 Torr, and temperature 302°K.

The $H^+$ signal seldom exceeded a few percent of that observed for $H_3^+$ and virtually vanished at gas pressures above 0.65 Torr. Figure 5 shows that the $H^+$ operational mobility data recorded below a value of $E/p_0$ less than about 5 V/cm Torr are independent of $E/p_0$. An average of these low-$E/p_0$ data yields a reduced, zero-field mobility of 16.0 cm²/V sec for $H^+$.

## VII. ION-MOLECULE REACTIONS

Figures 4 and 5 present operational mobility data which have been judged to represent essentially primary $H_3^+$ and $H^+$ ions. The display of $H^+$ data in Fig. 5 was terminated at an $E/p_0$ of 54 V/cm Torr because the $H^+$ arrival-time histograms indicated that, above this value of $E/p_0$, there was a growing contribution of secondary $H^+$ ions. Figure 6 shows an $H^+$ arrival-time histogram recorded at an $E/p_0$ of 56 V/cm Torr. Note that, when compared to the histograms in Figs. 2 and 3, the $H^+$ histogram exhibits an anomalous "toe." The main body of the histogram corresponds to the primary $H^+$ ions created in the electron-impact source; the toe represents

ions that were detected as $H^+$ but that had undoubtedly spent varying fractions of their drift time as a faster species. The position of the $H_3^+$ arrival-time histogram, which was recorded under the same conditions, leaves little doubt as to the identity of the faster species. Furthermore, no other hydrogen ions (or impurity ions) were present in the mass spectrum under these conditions. These secondary $H^+$ ions, which appear in growing numbers at increasing $E/p_0$, are apparently being formed by the breakup of the $H_3^+$ ion. Undoubtedly, this dissociation contributes to the mounting $H^+$ signal at increasing $E/p_0$, which was noted by Saporoschenko.[7]

Evidence for another hydrogen secondary process is shown by the example in Fig. 7, namely, the three-body conversion of $H^+$ into $H_3^+$ given by Eq. (5). The $H_3^+$ histograms recorded at gas pressures above 0.2 Torr show, when expanded, a small contribution from $H_3^+$ ions that spent fractions of their drift time as $H^+$ ions. These secondary $H_3^+$ ions contributed only negligibly to the total $H_3^+$ signal under the conditions of this investigation. Consequently, the computed mean arrival times could be justifiably ascribed to the vastly predominant primary $H_3^+$ ions.

Figure 8 presents an arrival-time histogram of $H_5^+$ ions, which were present in detectable quantities only

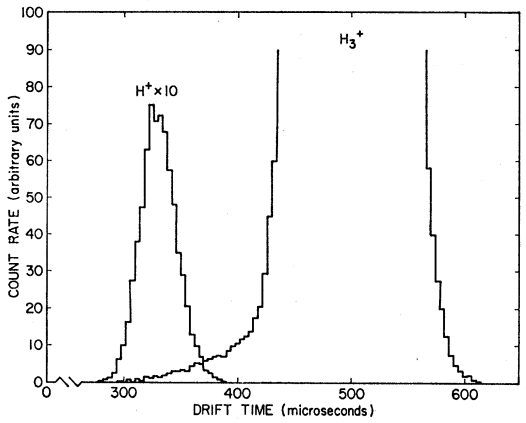


FIG. 7. A comparison between $H^+$ and $H_3^+$ arrival-time histograms recorded under the same conditions, with the latter showing contributions from the three-body conversion of $H^+$ into $H_3^+$ given by Eq. (5). The ratio of the $H_3^+$ signal to that of $H^+$ was 250. Drift distance 18.8 cm, pulse width 0.6 $\mu$sec, $E/p_0$ 5.0 V/cm Torr, pressure 0.35 Torr, and temperature 302°K.

at gas pressures above 0.65 Torr, and a histogram of $H_3^+$ ions taken under the same conditions. This example is typical of the comparisons obtained at a variety of experimental conditions. The coincident leading edges arise from the fact that these $H_5^+$ ions, which were formed very near the exit aperture, display the drift and diffusive characteristics of their $H_3^+$ progenitors. The trailing edge of the $H_5^+$ spectrum was always later than that of the $H_3^+$ ions, indicating that $H_5^+$ is the slower of the pair.

Clearly, a simple average of the $H_5^+$ arrival-time spectrum to obtain a drift velocity for $H_5^+$ ions alone would be erroneous.

## VIII. EXPERIMENTAL UNCERTAINTIES

The uncertainty in a value of the operational mobility arises from the error limits which must be assigned to the variables on the right side of Eq. (3); $v_d$, $E$, $p$, and $T$. A value for $v_d$ requires the determination of the quantities $\Delta L$ and $\Delta\bar{t}$, the distance between source positions and the difference in the two accompanying mean arrival times, respectively. The uncertainties in $\Delta L$, $E$, and $T$ are small in comparison to those in the other variables and are each estimated to be a few tenths of a percent. A comparison of the capacitance manometer with a symmetrically cold-trapped McLeod gauge suggested bounds of $\pm 2\%$ for the uncertainty of pressure measurements in the range $0.025 \leq p \leq 0.95$ Torr, the largest systematic uncertainty.

Possible errors in the determination of $\Delta\bar{t}$ are both random and systematic in nature. The random error in the measurement of the mean arrival time arises from the inability to maintain the experimental conditions precisely constant. As noted earlier, the variation of the points $(\bar{t}_i, L_i)$ about the fitted line from which $v_d$ was determined was a measure of this random uncertainty. The extreme of these variations was 2.5%, which is taken as a conservative bound on the random error in the determination of $\Delta\bar{t}$.

The systematic uncertainty in $\Delta\bar{t}$ stems from (a) possible errors in the time measurement itself ($\pm 1\%$) and (b) the fact that the ion swarm is sampled as a function of time rather than space. The latter arises in the following manner: If a drifting, thermal ion swarm, which had been created earlier by an instantaneous disk input of ions, were to be halted in flight and the

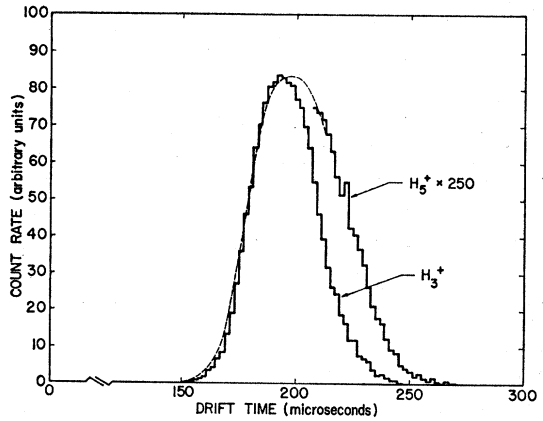


FIG. 8. A comparison between $H_3^+$ and $H_5^+$ arrival-time histograms recorded under the same conditions. The leading edge of the $H_5^+$ is represented by a smooth dashed line for clarity. Drift distance 6.3 cm, pulse width 0.5 $\mu$sec, $E/p_0$ 5.0 V/cm Torr, pressure 0.65 Torr, and temperature 303°K.

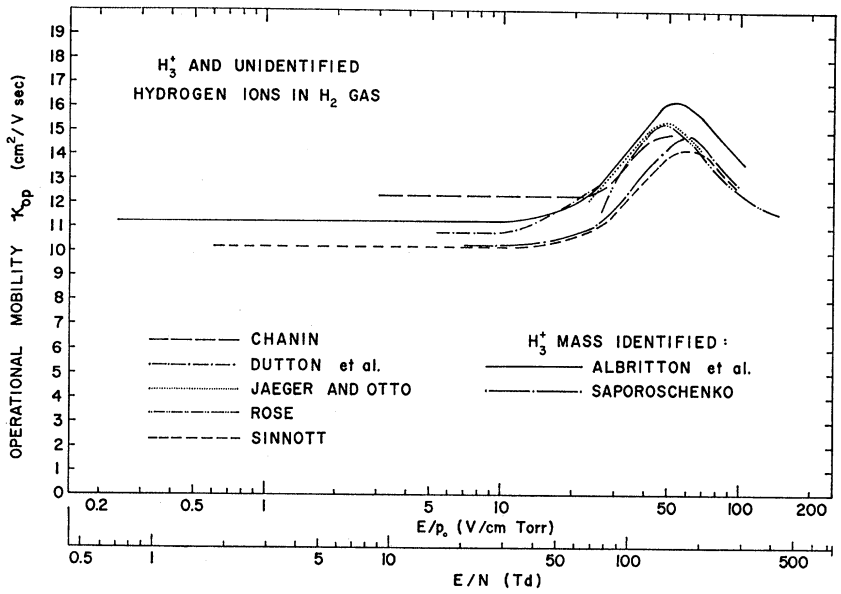


FIG. 9. A comparison between operational mobility data for mass-identified $H_3^+$ ions and unidentified hydrogen ions (presumed to be $H_3^+$) in hydrogen gas at room temperature. 1 Townsend (Td) $\equiv 10^{-17}$ V cm$^2$.

ion density sampled axially, the resulting spatial distribution would be Gaussian and centered about the position $v_d\bar{t}$. But it is necessarily the distance, rather than the time, which must be fixed. Hence, the trailing part of the swarm remains in the drift space longer than does the leading portion and has more time to diffuse. As a result, the arrival-time spectrum is a slightly skewed Gaussian (see Figs. 2 and 3), and the peak of the distribution is shifted to a time slightly earlier than $L/v_d$. Lowke[16] has explored the error in taking the peak of an arrival-time distribution to represent $L/v_d$. In the present investigation, Eq. (7) was used to examine the discrepancies between not only the peak of a spectrum, but also the first moment $\bar{t}$ and $L/v_d$ at low-$E/p_0$ conditions. It was found[17] that the first moment is a better approximation to $L/v_d$ than is the peak of a spectrum. The discrepancy between $\bar{t}$ and $L/v_d$ is very nearly proportional to the diffusion coefficient, and, at the pressures used in the present investigation, is less than 0.5%.

It is felt that these individual contributions of uncertainty call for $\pm 5\%$ error limits on the zero-field mobilities quoted herein. Equation (7) is strictly valid only when the ions are near thermal equilibrium; consequently, there is a shortage of tools with which one can investigate the high-$E/p_0$ region. Using the dependence of the error in $\Delta\bar{t}$ on the diffusion only as a guide, one can say that the observed[12] sharp increase of the components of the diffusion tensor at high $E/p_0$ could cause the measured values of $\mathcal{K}_{op}$ to be erroneously large. As a consequence, $\pm 10\%$ error limits are placed on the high-$E/p_0$ data.

To check the reasonableness of the above uncertainty limits and, perhaps more importantly, to demonstrate that the apparatus is free from any gross *unknown* systematic errors, the operational mobilities of potassium ions in hydrogen were measured. A pulsed source of $K^+$ ions was inserted into the electron-impact source structure. Otherwise, the apparatus was unchanged. Values of $\mathcal{K}_{op}$ were recorded for $K^+$ ions in the range $0.6 \leq E/p_0 \leq 51$ V/cm Torr, pressures $0.1 \leq p \leq 0.95$ Torr, and using the same techniques as were used for the hydrogen ions, as far as was possible. The resulting reduced, zero-field mobility of 12.9 cm$^2$/V sec compares well to the 12.7 cm$^2$/V sec reported by Tyndall[18] and to the $12.75 \pm 0.04$ cm$^2$/V sec recently measured by Elford,[19] who recorded data at pressures in the range 1–50 Torr in an apparatus employing electric shutters, but without positive mass analysis. The agreement with Elford's operational mobility data in the overlapping $E/p_0$ range was from 1–2%, with the present data slightly higher. The implication is that, except for sources of error *specifically* related to the hydrogen ions, the uncertainty estimates above reflect the proper magnitude of *known* possible error and include all significant sources of uncertainty.

## IX. PREVIOUS MEASUREMENTS ON HYDROGEN

Figure 9 permits comparisons between the results of the present investigation and those of others. The present value of $11.1 \pm 0.6$ cm$^2$/V sec for the reduced, zero-field mobility of $H_3^+$ agrees, within the combined error limits, with that obtained by Chanin, Dutton

[16] J. J. Lowke, Australian J. Phys. 15, 39 (1962).
[17] D. L. Albritton, Ph.D. dissertation, Georgia Institute of Technology, Atlanta, Ga., Appendix III, 1967 (unpublished).
[18] A. M. Tyndall, *The Mobility of Positive Ions in Gases* (Cambridge University Press, Cambridge, England, 1938).
[19] M. T. Elford, Australian J. Phys. 20, 471 (1967).

*et al.*, Saporoschenko, and Sinnott and stands in best agreement with the result of Dutton and coworkers. Not shown on the figure are the results of early investigations or the result of Oskam and Mittelstadt,[20] 13.3±0.5 cm²/V sec, deduced for an ion believed to be $H_3^+$ in afterglow studies. None of these values are in agreement with the theoretical prediction of Mason and Vanderslice,[21] 22.0 cm²/V sec, presumably because of the omission from the calculations of the proton exchange suggested by Varney.[4] The increase in $\mathcal{K}_{op}$ at an $E/p_0$ of about 10 V/cm Torr has been documented by several investigators, as well as the maximum near 50 V/cm Torr. Above this value, the present data are consistently higher than the data of others.

Figure 10 shows that the $H^+$ data of Saporoschenko gave no evidence of approaching a constant value as $E/p_0$ decreases, and as a result, no extrapolation to zero field strength is justified. Therefore, there is no drift tube measurement of the zero-field mobility of mass-identified $H^+$ ions with which the present value of 16.0±0.8 cm²/V sec may be compared. Oskam and Mittelstadt deduced a value of 16.4 cm²/V sec for the zero-field mobility of a "fast" ion in the hydrogen afterglow and surmised its identity to be $H^+$. The close comparison between this value and that obtained in the present investigation may be somewhat fortuitous in view of the dissimilar zero-field mobilities obtained for $H_3^+$. The theoretical predictions of Mason and Vanderslice for the zero-field mobility of $H^+$ considered all presently known modes of interaction between $H^+$ and $H_2$. Their prediction of 18.3 cm²/V sec stands in fairly favorable comparison (14%) to the experimental value of 16.0±0.8 cm²/V sec.

## X. CONCLUSIONS

The close fit between the experimental arrival-time histograms recorded at $E/p_0<10$ V/cm Torr and the spectra predicted by an appropriate model of thermal ionic motion demonstrate that $H_3^+$ may be considered a primary ion under low-$E/p_0$ conditions, despite its formation by the reaction of Eq. (4). Moreover, the slightly skewed Gaussian shapes of the histograms recorded at $E/p_0$ greater than 10 V/cm Torr strongly suggest that this conclusion may be extended to include the high-$E/p_0$ range. Finally, these facts support the conclusion that the reactions in Eqs. (5) and (6) only negligibly affect the $H_3^+$ data of the present investigation. The reduced, zero-field mobility of $H_3^+$ in hydrogen is 11.1±0.6 cm²/V sec.

At $E/p_0\leq 5$ V/cm Torr, the recorded arrival-time spectra of $H^+$ were those of primary ions alone. The zero-field mobility of $H^+$ in hydrogen is 16.0±0.8 cm²/V sec, in fair agreement with theoretical predictions. Above an $E/p_0$ of about 40 V/cm Torr, secondary

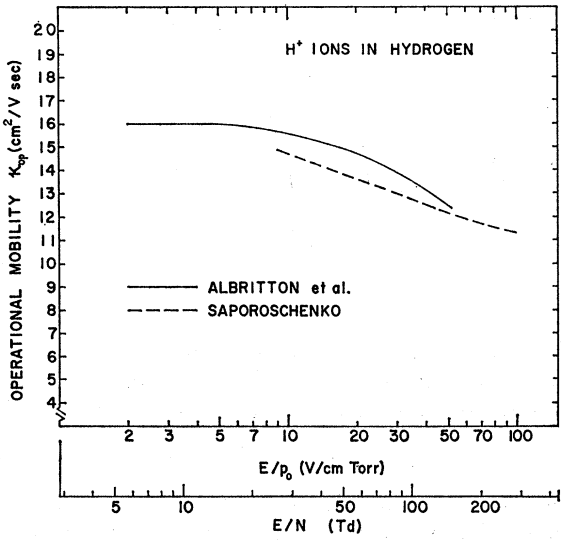


FIG. 10. A comparison between operational mobility data for mass-identified $H^+$ ions in hydrogen gas at 300°K (typical). 1 Townsend (Td) $\equiv 10^{-17}$ V cm².

$H^+$ ions are formed in increasing numbers by the disruption of $H_3^+$.

It is interesting to note that below an $E/p_0$ of about 30 V/cm Torr, $H^+$ is the faster ion and it is converted into $H_3^+$ via the process of Eq. (5). However, in the region above this value, $H_3^+$ is faster and it is here that one begins to observe the production of $H^+$ by the disruption of $H_3^+$.

$H_5^+$ is formed entirely by secondary processes and the straightforward, time-of-flight techniques described herein could not be used to measure its drift velocity.

## ACKNOWLEDGMENTS

The authors are indebted to Dr. Ian Gatland, who formulated the analysis in the Appendix, and to J. T. Moseley for his valuable assistance in making these measurements.

## APPENDIX

The continuity equation for the ionic number density is

$$\partial n/\partial t = D\nabla^2 n - v_d(\partial n/\partial z) + \beta(r,\theta,z,t). \quad (8)$$

The number density $n(r,\theta,z,t)$ refers to a single, nonreacting ionic species created entirely by the ion source, the output of which is represented by the source term $\beta(r,\theta,z,t)$. A cylindrical coordinate system has been chosen with the origin at the ion source and the $z$ axis in the direction of the electric field. The use of a scalar diffusion coefficient $D$ restricts the solution to low-$E/p_0$ values. This restriction is motivated by the fact that the components of the diffusion tensor at high $E/p_0$ are not known, whereas at low $E/p_0$, the diffusion

[20] H. J. Oskam and V. R. Mittelstadt, Physica **30**, 2021 (1964).
[21] E. A. Mason and J. T. Vanderslice, Phys. Rev. **114**, 497 (1959).

coefficient may be calculated from the measured mobility $K$ via[22]

$$D/K=kT/e, \tag{9}$$

where $k$ and $e$ are the Boltzmann constant and the ionic charge, respectively. The general solution of Eq. (8) in an infinite volume is

$$n(r,\theta,z,t)=\int_0^\infty r'dr'\int_0^{2\pi}d\theta'\int_{-\infty}^{\infty}dz'\int_{-\infty}^{t}dt'\left\{\frac{\beta(r',\theta',z',t')}{[4\pi D(t-t')]^{3/2}}\times\exp\left[-\frac{r^2+r'^2-2rr'\cos(\theta-\theta')+[z-z'-v_d(t-t')]^2}{4D(t-t')}\right]\right\}. \tag{10}$$

The ion source in the present apparatus creats an axially thin, uniform disk of ions at $t=0$, $z=0$ and its azimuthally symmetric output may be approximated by

$$\beta(r,z,t)=\sigma_0 H(r_0-r)\delta(t)\delta(z), \tag{11}$$

where $\sigma_0$ is the initial ionic surface density, $r_0$ is the radius of the ion source aperture, and $H(x)$ is the Heaviside step function: $H(x<0)\equiv 0$, $H(x>0)\equiv 1$. With this form for the source term, the integration of Eq. (10) yields

$$n(r,z,t)=\frac{\sigma_0}{(4\pi Dt)^{1/2}}\exp\left(-\frac{(z-v_d t)^2}{4Dt}\right)\times\left[1-\sum_{l=0}^{\infty}\sum_{m=0}^{l}\frac{1}{l!}\frac{1}{m!}\times\exp\left(-\frac{(r^2+r_0^2)}{4Dt}\right)\left(\frac{r^2}{4Dt}\right)^l\left(\frac{r_0^2}{4Dt}\right)^m\right]. \tag{12}$$

Since the ions detected in this apparatus are those which leave the drift tube through a central exit aperture, the desired expression for the number density is Eq. (12) evaluated at $r=0$:

$$n(0,z,t)=\frac{\sigma_0}{(4\pi Dt)^{1/2}}\exp\left(-\frac{(z-v_d t)^2}{4Dt}\right)\times\left[1-\exp\left(-\frac{r_0^2}{4Dt}\right)\right]. \tag{13}$$

The quantity that is actually measured is the ionic flux through the exit aperture, $\varphi=AJ_z$, where $J_z$ is the $z$ component of the ionic particle current density at the aperture of area $A$, or

$$\varphi=A[-D(\partial n/\partial z)+v_d n]. \tag{14}$$

It follows that the time variation of the sampled flux is given by

$$\varphi(0,z,t)=\frac{A\sigma_0}{4(\pi Dt)^{1/2}}(v_d+z/t)\exp\left(-\frac{(z-v_d t)^2}{4Dt}\right)\times\left[1-\exp\left(-\frac{r_0^2}{4Dt}\right)\right]. \tag{7}$$

[22] E. W. McDaniel, *Collision Phenomena in Ionized Gases* (John Wiley & Sons, Inc., New York, 1964), p. 491.